

Research Article

Temporal and Spatial Evolution Mechanisms of the Water-Conducting Fractured Zone of Overlying Strata in the Kongzhuang Coal Mine

Zhang Pei-ding,¹ Sun Chao-shang,¹ Fan Xuan,² Li Song-tao,² Wang Long-jing,² and Cao Zheng-zheng^{3,4} 

¹Shanghai Datun Energy Resources Co., Ltd., Xuzhou, 221000 Jiangsu, China

²School of Energy Science and Engineering, Henan Polytechnic University, Jiaozuo, 454000 Henan, China

³Henan Mine Water Disaster Prevention and Control and Water Resources Utilization Engineering Technology Research Center, Henan Polytechnic University, Jiaozuo, 454000 Henan, China

⁴Collaborative Innovation Center of Coal Work Safety and Clean High Efficiency Utilization, Collaborative Innovation Center of Advanced Microstructures, Jiaozuo, 454000 Henan, China

Correspondence should be addressed to Cao Zheng-zheng; hpu_zzc@126.com

Received 8 August 2022; Revised 21 December 2022; Accepted 10 June 2023; Published 21 June 2023

Academic Editor: Liang Xin

Copyright © 2023 Zhang Pei-ding et al. This is an open access article distributed under the Creative Commons Attribution License, which permits unrestricted use, distribution, and reproduction in any medium, provided the original work is properly cited.

Kongzhuang coal mine of Shanghai Datun Energy Resources Co., Ltd. is a typical deep coal mine in eastern China. The mining disturbance of working face in deep coal mine leads to the fracture and movement of overlying strata and the damage of the aquifer in overlying strata, thereby causing water inrush disaster and posing a serious threat to the safety production in coal mine. Therefore, the temporal and spatial evolution mechanism of the water-conducting fractured zone of overlying strata in the Kongzhuang coal mine is researched systematically in this paper. Especially, the hydro-geological conditions and mining conditions in the Kongzhuang coal mine are analyzed; on this basis, the fracture and movement of overlying strata are simulated by physical similarity simulation test, and the temporal and spatial evolution rule of overlying strata in the Kongzhuang coal mine is obtained. Besides, the development height of “two zones” is measured by double-end water shutoff detection method, and the risk assessment for the water inrush disaster of the coal seam roof is carried out in the Kongzhuang coal mine. The research achievements in this paper indicate that the water-conducting channel formed in the mining process of #7 coal seam is the most important water-filling channel. Quaternary aquifer water recharges the mine indirectly through the bedrock aquifer, and the sandy mudstone with large thickness is the key layer to control the development of a water-conducting fracture zone. Meanwhile, the height of the caving zone is 26.7 m, about 8.3 times of mining height, and the height of the fracture zone is 68.3 m, approximately equal to 16.26 of the mining height. The results of #1 and #2 borehole leakages in the double-end water shutoff detection method show that the height of the water-conducting fractured zone is 63.70 m–65.27 m, and the split-to-mining ratio is 15.17–15.54. The water inrush risk of the coal seam roof shows that most of the 7436 working face is in the transition zone, and a small area around the cutting hole of the working face is in the relatively dangerous zone. Therefore, the innovation of this paper is that the temporal and spatial evolution mechanism of the water-conducting fractured zone of overlying strata in the Kongzhuang coal mine is revealed, which provides the theoretical guidance for the prediction and prevention of water inrush disaster in the coal mine with the similar mining conditions.

1. Introduction

In recent years, shallow coal mine resources in eastern China have gradually dried up and exhausted, while deep mine

resources are extremely rich, so the mining situation changes gradually from shallow mining to deep mining [1–3]. At present, the buried depth of the coal seam extraction in China increases at a rate of approximately 20 m per year.

Additionally, many coal mines are at a depth of more than 1000 m, exceeding the initial conceptual depth. The typical characteristics of coal mining in deep coal mine are high ground stress, high ground temperature, high osmotic pressure, and large mining disturbance [4–6]. Among them, high in situ stress can easily cause issues such as floor heave, roof collapse, and water inrush disaster.

For example, the Kongzhuang coal mine of Shanghai Datun Energy Resources Co., Ltd. is one of the typical deep coal mines. There are multilayer thick sandstone key layers in the roof of the deep working face, and the key layer breaking is the key factor leading to the water dynamic load disaster of top layer separation, which has an adverse effect on safety production [7–9]. Therefore, it is necessary to analyze the water-rich aquifer of the roof in the Kongzhuang coal mine, the fracture characteristics of key layers, and the height of “two zones”. Specifically, the “two zones” refers to the caving zone and fractured zone in overburden [10]. The characteristics and evolution rule of roof water inrush in the Kongzhuang coal mine are studied in this paper.

Many scholars have studied the development law of the water-conducting fracture zone and the control effect of the main key layer on the water-conducting fracture zone. For example, Xu et al. [11] studied the impact of the location of the primary key stratum on the evolution range of water-flowing fracture, by adopting theoretical analysis, simulation experiment, and engineering exploration, which were employed to conduct the water inrush protection in Bulianta coal mine, Shendong coal field. Shi et al. [12] described a drift model of water migration along the working face below a roadway and found that “zebra fractures” provided the main passageway for water where large amounts of water inrush occurred through the roof. Based on depth study of the influence law of key strata on the height of fractured water-conducting zone, Xu et al. [13] proposed a new method to predict the height of fractured water-conducting zone by location of key strata and distinguished the abnormal development of the height of fractured water-conducting zone induced by structural changes of key stratum, which was verified by engineering measurements results. Chen et al. [14] studied the correlation of roof water-gushing and roof movement law by the methods of theoretical analysis and field measurement and put forward that roof water gush was predicted and controlled, according to the water abundance and the law of roof fracturing instability. Based on the occurrence features of the extrathick seam and water-rich overburden in the Binchang mining area, Gao et al. [15] analyzed the failure characteristics of Luohe thick sandstone aquifer under high-strength mining by using the numerical simulation method and proposed the water inrush danger and comprehensive control technology consisting of height permitted mining and depressurizing. In terms of the conditions of missed or thin coal seam direct roof impermeable layer and poor water yield capacity of roof aquifer, on the basis of the “three maps-two predictions” method, the roof aquifer water-bursting risk evaluation method was further investigated by Wu et al. [16] from two aspects, one was roof caving and fractured degree, and the other was roof aquifer water yield capacity. Accord-

ing to the calculated height of the water-conducting zone, the safety of roof cracking was partitioned by Zeng et al. [17], and the calculation formula for the height of the water-conducting fractured zone was obtained which accords with the actual situation of the study area. Then, the risk of water inrush from the bedrock aquifer of the coal seam roof was evaluated by combining with the result of the water abundance evaluation. Sun et al. [18] determined the water source of the mine roof surge in a minefield in the Shaanxi Jiaoping mining area, by the method of water quality analysis and the development height analysis of the water-conducting fracture zone; besides, on the basis of the water-rich analysis based on the GI-variation coefficient method risk analysis of the separation development, the risk of roof water inrush was evaluated by superposition analysis. Based on the type partition of water-conducted fracture and the mechanical analysis of seepage flow or pipe flow model, Cao et al. [19] studied the distribution model of water-conducted fracture main channel and built the distribution model of water-conducted fracture main channel in the light of the breaking size of key strata, which provided a theoretical basis to the implementation of artificial control on the water flow in the main channel of water-conducted fractures. Du et al. [20] explored the internal response relationship between the development of fracture zone and optical fiber detection data by applying the distributed optical fiber sensing technology to the similarity model test and established the internal relationship between the shapes of the strain curve, the development height of water conducted fracture zone, and the activity of key stratum. Yun Zhang et al. [21] proposed the short-wall block coal mining technology and studied the development law of water-conducting fracture zone in overburden during short-wall mining, providing an important reference for improving the recovery rate of coal resources and optimizing the mining theory of water resources protection. Zheng et al. [22] used FLAC3D finite element software to simulate and analyze the size effect of the height of the water-conducting fracture based on the characteristics of overlying rock in the Xinzhuang coal mine, indicating that the height of the water-conducting fracture zone was positively correlated with the increase of mining thickness and working face width. Zhang et al. [23] analyzed the relationship between the height of a water-conducting fracture zone and each single influencing factor by using the method of multiple regression analysis and analyzed the fitting formula of the height of a water-conducting fracture zone and each factor by using multiple nonlinear regression analysis.

It is obvious that the development law of the water-conducting fracture zone and the control effect of the main key layer on the water-conducting fracture zone has been researched widely in previous research achievements. However, the temporal and spatial evolution mechanism of water-conducting fractured zone of overlying strata in deep coal mine, such as the Kongzhuang coal mine, is not obtained, which should be researched systematically, on the basis of those research achievements. Therefore, the hydrogeological conditions and mining conditions in the Kongzhuang coal mine are analyzed in this paper. The state

of rock caving and the change of stress in the process of mining are studied by similarity simulation test. Finally, the development height of the “two zones” of overlying rock in the deep working face is detected by double-end water shutoff device, thus providing theoretical guidance for water disaster prevention and control in the Kongzhuang coal mine.

2. Geological Conditions and Mining Conditions

Kongzhuang coal mine is located in Xuzhou City, Jiangsu Province, China, which is attached to Shanghai Datun Energy Resources Co., Ltd. The 7303 fully mechanized working face is located in the middle and upper part of the III5 mining area in the Kongzhuang coal mine. The working face has a -760 m contour line in the north, a chute of 7301 working face in the south, a KF13 fault in the East, and pedestrian downhill of the III5 mining area in the West. Obviously, the 7303 fully mechanized working face in the Kongzhuang coal mine is a typical working face in the deep coal mine. The elevation of the working face is +33.38 m corresponding to the ground elevation, and the elevation of the working face is -641.6~-764.7 m. The strike length of the working face is 1015 m, and the dip length is 205 m. The thickness of #7 coal seam is 2.90~5.00 m, with an average thickness of 3.20 m. The coal seam dip angle of the working face is 15°~25°, and the average dip angle is 19°. The roof of the coal seam is mudstone, the main roof is fine sandstone, and the direct bottom is fine sandstone.

The main water filling sources affecting #7 coal mining in the deep Kongzhuang coal mine are sandstone water at the boundary of the Lower Shihezi Formation and sandstone fissure water at the roof of the Shanxi Formation. #7 coal roof sandstone fissure aquifer has poor and uneven fissure development, the overall water yield is weak, and the water yield in the deep part is worse than that in the shallow part, where the distance between the sandstone aquifer at the bottom of the Lower Shihezi Formation and coal seam 7 is small; the water-conducting fracture zone may affect this layer.

In addition, the water-filling channel formed by mining activities has become the most important water-filling channel for mine water filling [24–26]. The Quaternary bottom aquifer water may indirectly fill the mine by supplying the bedrock aquifer, so that the bedrock aquifer also becomes a channel for mine water filling. Through the identification of key layers in 24-47 boreholes of 7303 working face, the results show that coarse sandstone (7.71 m) 64.76 m away from #7 coal is the main key layer, and mudstone (5.93 m), mudstone (6.56 m) 27.75 m away from #7 coal, and mudstone (7.65 m) 35.94 m away from 7 coal are subkey layers. The sandy rock stratum is thin, and the sandy mudstone with a large thickness has an obvious control effect on the development of water-conducting fracture zone.

3. Physical Similarity Simulation of Overburden Failure

3.1. Physical Similarity Simulation Test. The physical similarity simulation test is an important research method to research the overburden failure in deep mining, and the the-

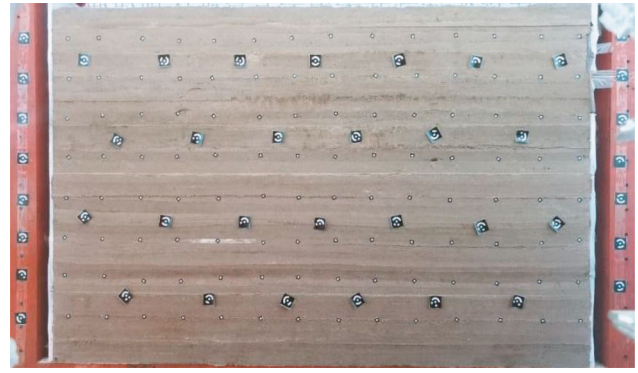


FIGURE 1: Layout of the model survey line.

oretical principle of the physical similarity simulation test is the geometric similarity, movement similarity, and dynamic similarity. The test is carried out on the 2750 mm × 1900 mm × 320 mm (length × height × width) specification test table. The design model has a height of 1900 mm, a coal thickness of 32 mm, and a bottom plate thickness of 100 mm. In order to study the characteristics of overburden fracture and migration and the development height of water-conducting fracture zone during the excavation of #7 coal seam in Kongzhuang coal mine. The physical similarity model is built and excavated along the coal seam trend. Besides, the physical similarity model is excavated step by step, and the 30 cm protective coal pillars are reserved on both sides. A total of 215 cm is excavated, which is equivalent to 215 m advance of the working face.

In order to observe the displacement change of overburden during the advance of the working face, a total of 8 survey lines are arranged along the coal seam roof from bottom to top. Survey line 8 is 10 cm from the coal seam roof, survey line 7 is 30 cm from the coal seam roof, survey line 6 is 50 cm from the coal seam roof, survey line 5 is 70 cm from the coal seam roof, survey line 4 is 90 cm from the coal seam roof, survey line 3 is 110 cm from the coal seam roof, survey line 2 is 120 cm from the coal seam roof, and survey line 1 is 140 cm from the coal seam roof. Each measuring line is arranged with 14 measuring points along the mining direction of the coal seam, and the distance between adjacent measuring points is 20 cm. A total of 112 displacement measuring points are arranged in the whole model. The layouts of displacement measuring points and working face are shown in Figures 1 and 2.

During the process from the opening of the cutting hole to the mining of 215 cm, the model is excavated step by step, and each mining is 4 cm, which is equal to the advance of the actual working face by 4 m. One-time excavation directly exploits 215 cm, which is equal to the 215 m length of the actual working face. During the excavation, the fracture characteristics and fracture development of the upper overburden are observed and recorded, and the movement of the upper overburden is monitored by a digital camera. Then, through computer image processing technology, the digital image is processed, and the change with the overall displacement of the overlying strata in the mining face is analyzed. The last measurement is carried out after the completion of all simulated mining and the stability of strata movement.

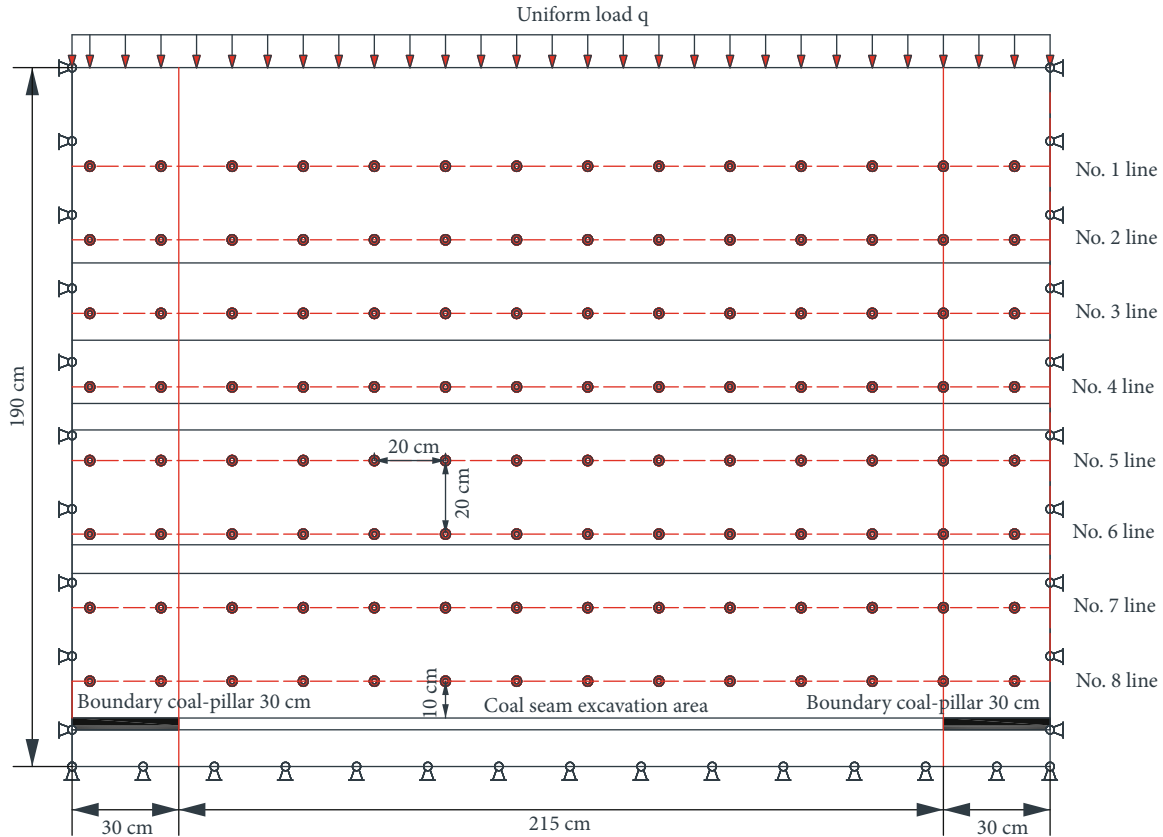


FIGURE 2: Schematic diagram of displacement measurement points of strike model.

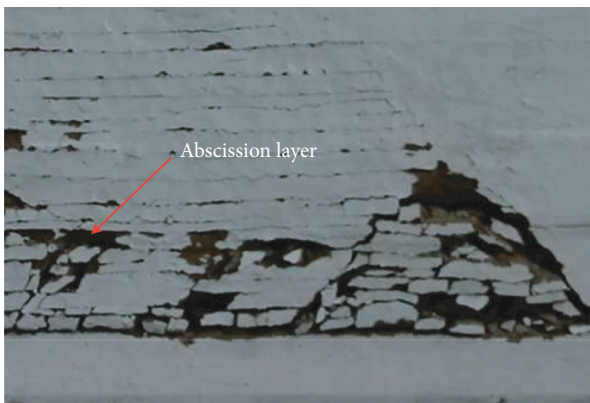


FIGURE 3: Characteristics of caving zone.

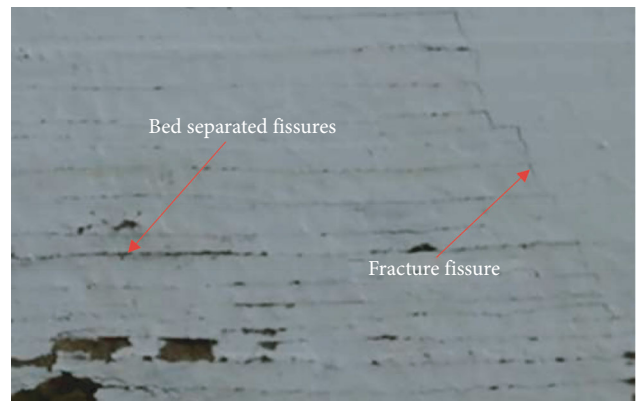


FIGURE 4: Characteristics of the fracture zone.

According to the analysis of overburden collapse form with different advancement distances, there are 11 cycles of roof periodical weight and the average roof weight step is 16m in this experiment. In the process of coal seam excavation, under the action of roof periodical weight, the roof of the working face has experienced separation, fracture, and fracture in the overall test process, and then a collapse zone is generated. The collapse zone is roughly trapezoidal, and its characteristics are shown in Figure 3. With the continuous advance of the working face, many longitudinal and separated fractures appear in the overlying strata of the main roof. The formation of a water-

conducting fracture zone develops from low speed to high speed, and the separation layer fracture presents a dynamic change process of generation, expansion, contraction, and closure, shown in Figure 4.

It is obvious that the water-conducting channel of the overlying water-bearing rock layer is difficult to pass through the separation crack, because the separation cracks shrink and close with the advance of the working face, so as to gradually compact. The water-conducting channel is mainly composed of rock fracture, so the development of fracture is restrained through the implementation of corresponding measures in actual production, shown in Figure 5.



FIGURE 5: Main water channels in the fracture zone.

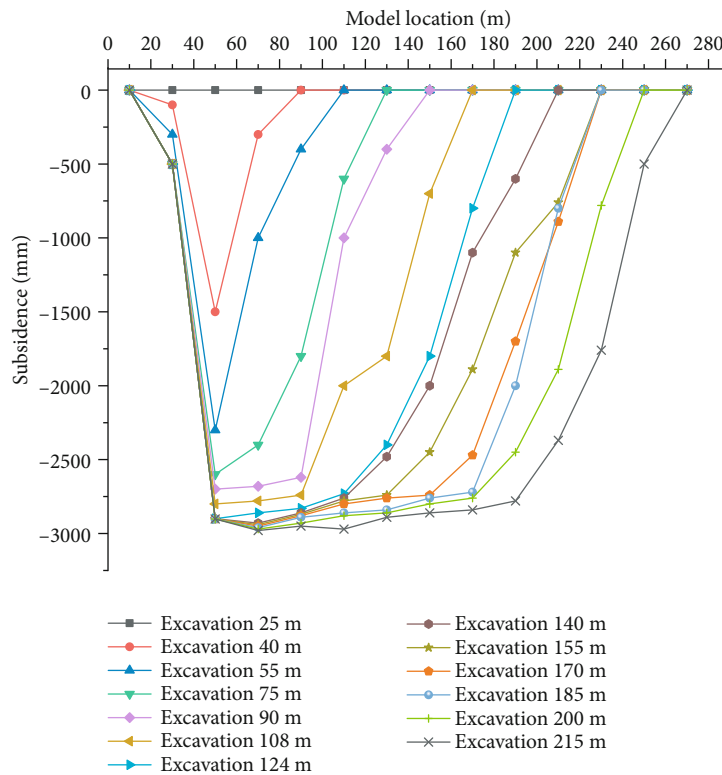


FIGURE 6: Vertical displacement curve of line 8.

With the advancement of the working face, the water-conducting fractured zone develops upward. In order to intuitively reflect the relationship between the water diversion fracture zone and the advancing distance of the working face, the distribution curve of the water diversion fracture zone and the advancing distance of the working face are drawn according to the test data. After the work-

ing face advances to 108 m, the development height of the water-conducting fracture zone increases significantly. The specific reason is the large-scale collapse of the roof at this time. Therefore, the development of fissures is suppressed by the implementation of corresponding measures in actual production. When the working face advances to 155 m, the water-conducting fractured zone develops to

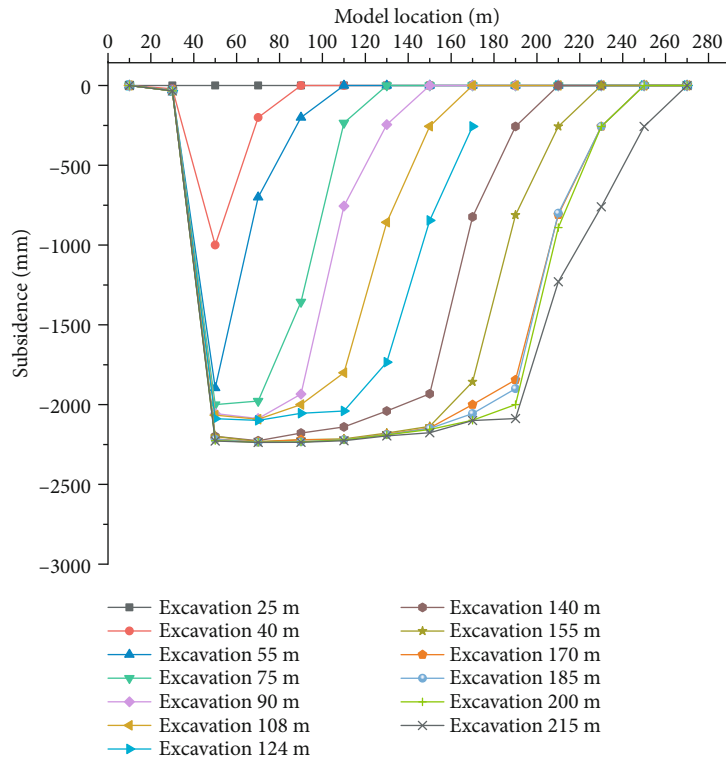


FIGURE 7: Vertical displacement curve of line 7.

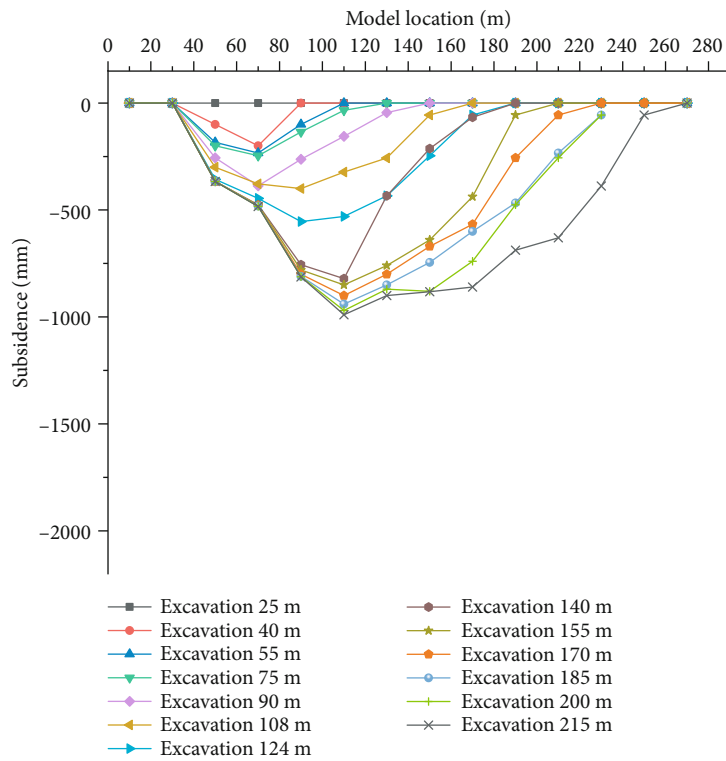


FIGURE 8: Vertical displacement curve of line 6.

the key stratum, and the development height of the water-conducting fractured zone is stable at about 78.3 m and does not continue to develop upward. It shows that the

maximum development height of the water-conducting fracture zone is about 78.3 m, which is 24.5 times of the coal thickness.

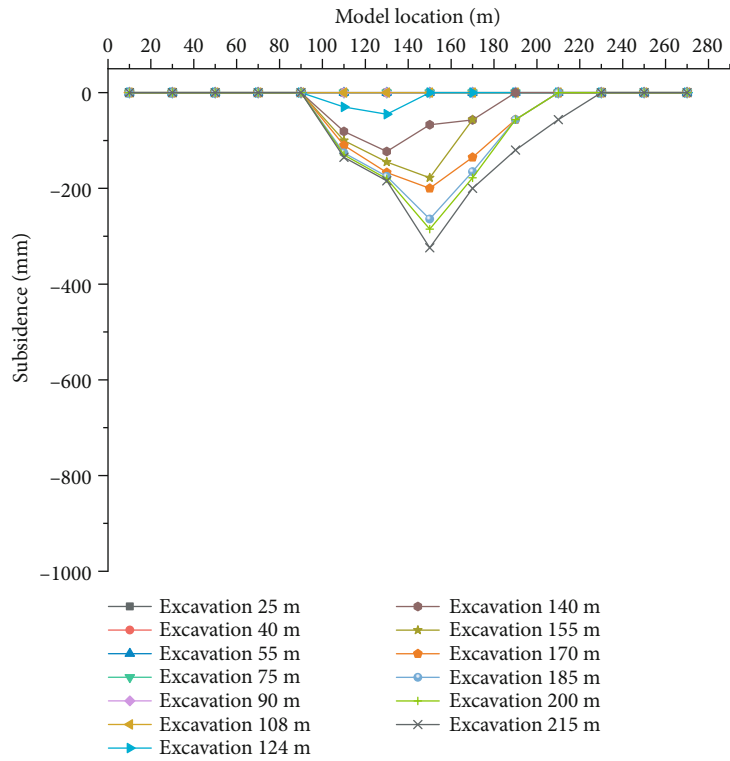


FIGURE 9: Vertical displacement curve of line 4.

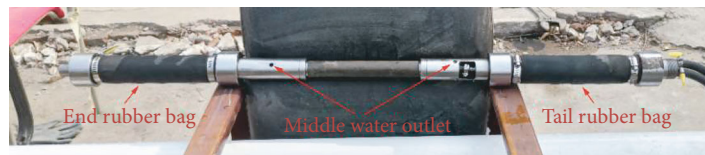


FIGURE 10: Double-end water shutoff.

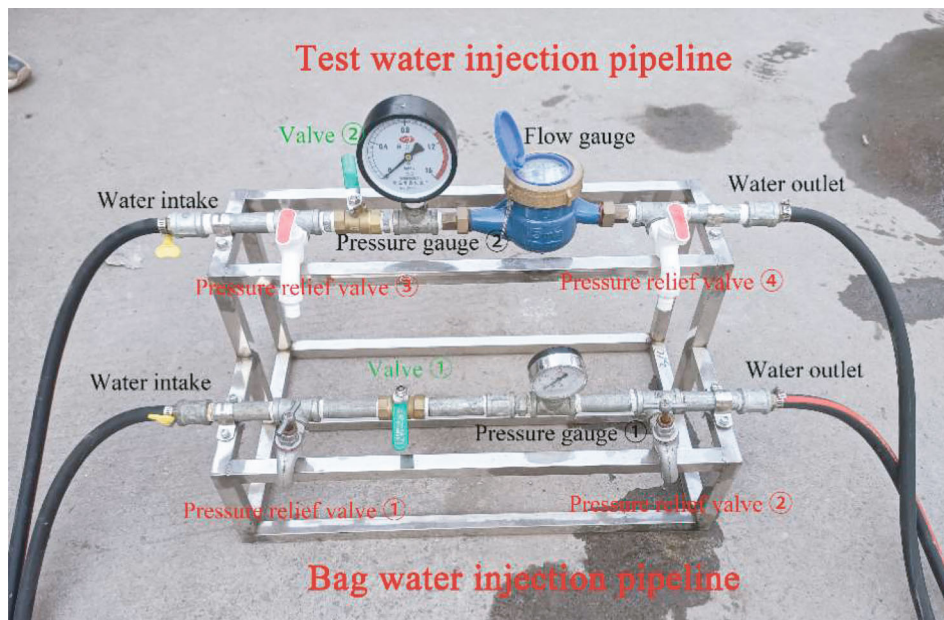


FIGURE 11: Water injection system.

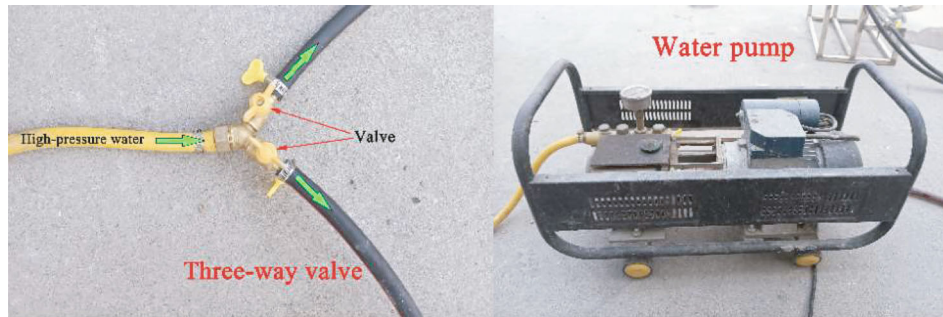


FIGURE 12: Three-way valve and water injection pump.



FIGURE 13: Water injection hole and tail connector of a double-end water shutoff.

3.2. *Analysis of Displacement Law of Overburden.* The change curve of vertical displacement of survey line 8 during coal seam excavation is shown in Figure 6. The vertical distance between the survey line 8 and the roof of the coal seam is 10 m. Before the first roof weight occurs in the working face, measuring line 8 is only slightly deformed. With the excavation of the coal seam, the measuring point on the direct top caving line 8 produces a large displacement. With the increase of the excavation distance of the working face, after the measuring point in the middle of the survey line reaches the maximum subsidence, there is no obvious change, indicating that the collapsed roof is gradually compacted in the process of advancing. When the working face is excavated to 215 m, the maximum subsidence of survey line 1 is 2.98 m.

The variation curve of vertical displacement of survey line 7 during coal seam excavation is shown in Figure 7. The vertical distance from line 7 to the roof of the coal seam is 30 m. The subsidence of survey line 7 is generally lower than that of survey line 8, and the subsidence space of the strata becomes smaller due to the collapse of the strata. After the working face is advanced to 155 m, the measuring point in the middle of survey line 7 basically does not deform after reaching the maximum subsidence, which indicates that the lower strata are gradually compacted after advancing to 155 m. When the working face is excavated to 215 m, the maximum subsidence of survey line 1 is 2.36 m.

The variation curve of vertical displacement of survey line 6 during coal seam excavation is shown in Figure 8. The vertical distance between line 6 and the roof of the coal seam is 50 m. Before the working face is advanced to 550 m, survey line 3 is only slightly deformed, indicating that the mining dynamic disturbance has not affected 50 m before advancing to 230 m. When the working face is advanced to 140 m, the

vertical displacement value of survey line 6 changes greatly, and the maximum subsidence displacement is 0.82 m at this time, which indicates that the overburden caving zone is further compacted by the overlying strata, and the roof collapses in a large range, resulting in the rapid upward development of the overlying strata fissures, while the bedding fissures in the middle overburden gradually begin to be compacted and closed. In the process of gradually advancing to 215 m, due to the periodic breaking of the overlying strata, the vertical displacement survey line changes in stages, and the final maximum subsidence value is 0.99 m.

The variation curve of vertical displacement of survey line 4 during coal seam excavation is shown in Figure 9. The vertical distance between survey line 5 and the roof of the coal seam is 90 m. The overall subsidence of survey line 4 changes slightly. When survey line 4 is excavated to 155 m in the coal seam, the subsidence amount gradually increases. When the coal seam is excavated to 215 m, the subsidence amount does not change greatly, and the final maximum subsidence value is 0.32 m. Therefore, when the coal seam under survey line 4 is excavated to 155 m, only delamination cracks occur, but no breakage occurs.

4. Development Height Measurement of “Two Zones” in Overburden

4.1. *Instructions of Double-End Water Shutoff.* The double-end water shutoff detection method is an important method to measure the development height of water-conducting fractured zone in overlying strata, which contains two rubber bags at the end and tail, and a water outlet hole in the middle, and the tail is connected to the water injection system through a high-pressure water pipe, as shown in Figure 10. Specifically, the double-end water shutoff

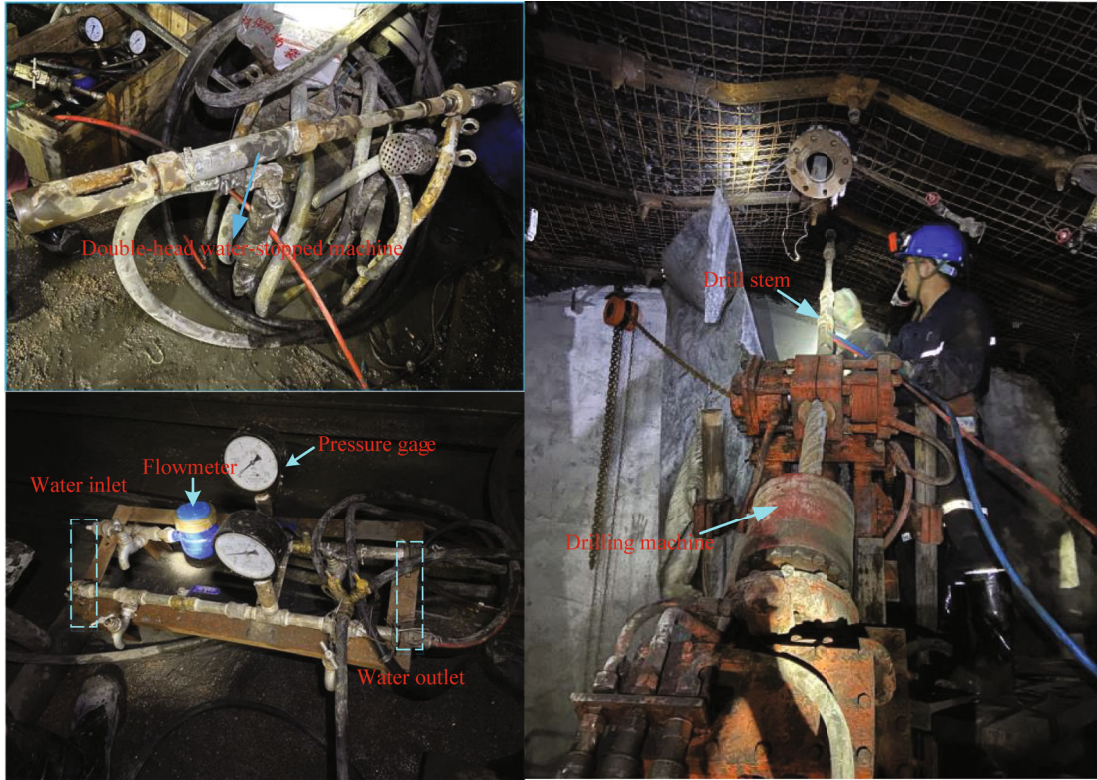


FIGURE 14: Field measurement of water-conducting fissure zone.

detection method is employed to select the appropriate detection site around the working face to dig and drill and to drill the inclined hole above the gob [27–30]. Besides, for the sake of obtaining the upper limit height of the water-conducting fractured zone, the double-end water shutoff device is employed to seal the borehole with water injection in different sections, and the leakage flow of each section of the borehole is measured.

The water injection system includes a bag water injection pipeline and test water injection pipeline, as shown in Figure 11. The water in the bag water injection pipeline passes through the inlet pressure relief valve ①, valve ①, pressure gauge ①, and pressure relief valve ② and, finally, enters the bag of the double-end water shutoff through the outlet pipeline; the water in the bag water injection pipeline passes through the water intake through pressure relief valve ③, valve ②, pressure gauge ②, flow gauge, and pressure relief valve ④ and, finally, through the water outlet pipeline into the middle of the double-end water shutoff device.

The water injection system outputs high-pressure water from a pump (directly supplied by a high-pressure water pipe downhole) [31–33]. A three-way valve is used to supply high-pressure water to the bag water injection pipeline and the test water injection pipeline, as shown in Figure 12.

The white hole at the tail of the double-end water shutoff is the test water injection hole, and the silver hole is the bag water injection hole. The tail of the double-end water shutoff is connected to the drill pipe using self-made connecting parts, as shown in Figure 13.

TABLE 1: Height of water-conducting fracture zone detected at working face 7303.

Hole number	Height of water-conducting fracture zone/m	The ratio of fracture height-to-recovery thickness
#1 hole	65.27	15.54
#2 hole	63.70	15.17

4.2. *Downhole Observation Process.* The self-designed double-end water shutoff device is used to monitor the water leakage of boreholes before and after mining and determine the distribution of fractures in each rock layer after mining. The system is composed of double-end water shutoff, pressure hose, observation platform, and so on. The observation equipment and downhole observation are shown in Figure 14. Borehole #2 was observed on January 14, 2022, followed by borehole #1 on April 22 and borehole #4 on April 23. During the observation of borehole #4, it is found that a certain amount of water flows out of the equipment, which is believed to be the rupture of the bag during the propulsion process.

4.3. *Detection Results Analysis.* When the overlying strata of the working face are not damaged, the change of the average water injection flow rate of premining contrast hole #4 is about 7.34 L/min due to the rupture of the double-end water shutoff bag in the field test. According to the field observation, there is a large leakage at the hole depth of 78 m, and

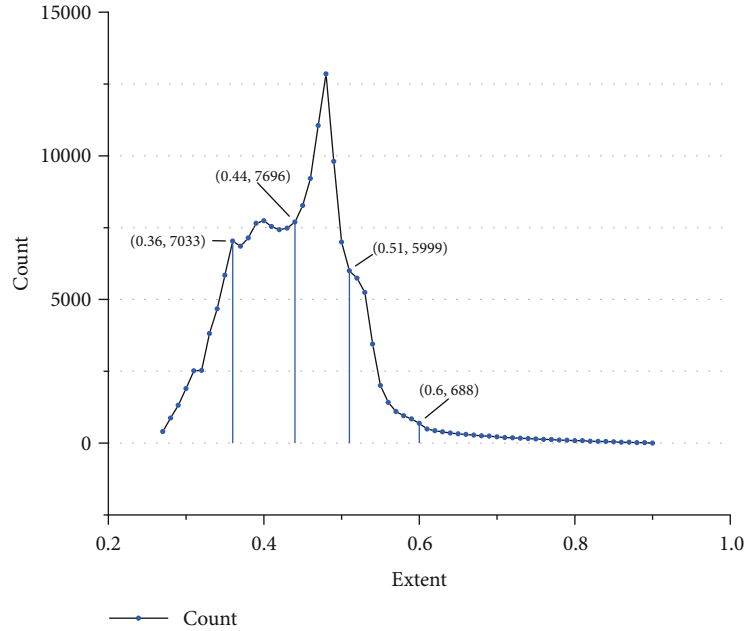


FIGURE 15: Natural grading diagram.

TABLE 2: Danger zone table of water intrusion.

Roof type area	Water inrush risk index (TS)
Safe area	<0.36
Safer area	(0.36, 0.44)
Transition area	(0.44, 0.51)
More dangerous areas	(0.51, 0.60)
Danger zone	>0.60

the leakage is up to 36.2 L/min. This is because the crack developed ahead of the detection area of contrast hole #4, and according to the results of the physical similarity simulation test, there is a separation of mudstone at 64.55 m away from the #7 coal seam.

The water injection loss in the 79.5~84 m range of the #1 borehole fluctuates in the range of 5.75~6 L/min. The comparison with the water injection leakage in the corresponding section of the #4 comparative hole shows that the stratum in this section is not damaged; the water injection leakage increases in the range of the hole depth of 46.5 m~78 m, which is significantly higher than that in the previous section, and the leakage reaches 5.5~10.6 L/min, indicating that this segment is the top of the water-conducting fracture zone. Therefore, the position of the water-conducting fracture zone in the overlying strata determined by the #1 hole is 78 m deep, the corresponding rock layer is 9.97 m thick mudstone, and the vertical height from the coal seam roof is 65.27 m.

The leakage of water injection in hole #2 shows that the leakage fluctuates in the range of 0.2 to 2.3 L/min in the range of hole depth of 81.5 to 95 m. The comparison with the leakage of the corresponding section of the #4 contrast hole shows that the stratum in this section is not damaged; the leakage of water injection in the range of the hole depth

of 72.5 m~80 m is significantly higher than that of the previous section, and the leakage reaches 0.75~10.65 L/min, indicating that this section is a water-conducting fracture with top. Since the water injection loss in this section increases rapidly, the rock formation has been seriously damaged from this section, and it has entered the water-conducting fissure zone. Therefore, the position of the top boundary of the water-conducting fracture zone of the overlying strata determined by the #2 hole is the hole depth of 80 m, and the vertical height from the top of the coal seam is 63.7 m.

To sum up, after the mining of the working face, the overlying strata are affected by the mining, resulting in a large number of new fractures. The leakage of the #1 hole is 5.5~10.6 L/min; #2 drilling loss is generally less than #1 drilling. The leakage of the #4 comparative hole is 7.34~36.2 L/min. During the construction, the bag of the double-ended water plug is ruptured, resulting in a large leakage. According to the similar simulation test results, the mudstone at a distance of 64.55 m from the #7 coal produces separation. Combined with the advanced fracture development mechanism, the phenomenon of large leakage at the hole depth of 78 m is reasonably explained. It is obvious that the maximum water-conducting fracture height measured in the 7303 working face is in the range of 63.70~65.27 m, and the fracture-mining ratio is 15.17:15.54, as shown in Table 1.

4.4. Water Inrush Risk Assessment Division. The evaluation model of the roof water inrush risk index in the no. 7 coal seam based on AHP has been established. Using the powerful spatial data analysis function of GIS, each thematic map is superimposed and calculated, and the thematic map of the water inrush risk index value of the coal seam roof is obtained [34–38]. Using the natural breaks method, the water inrush risk (TS) value of each grid in the coal seam

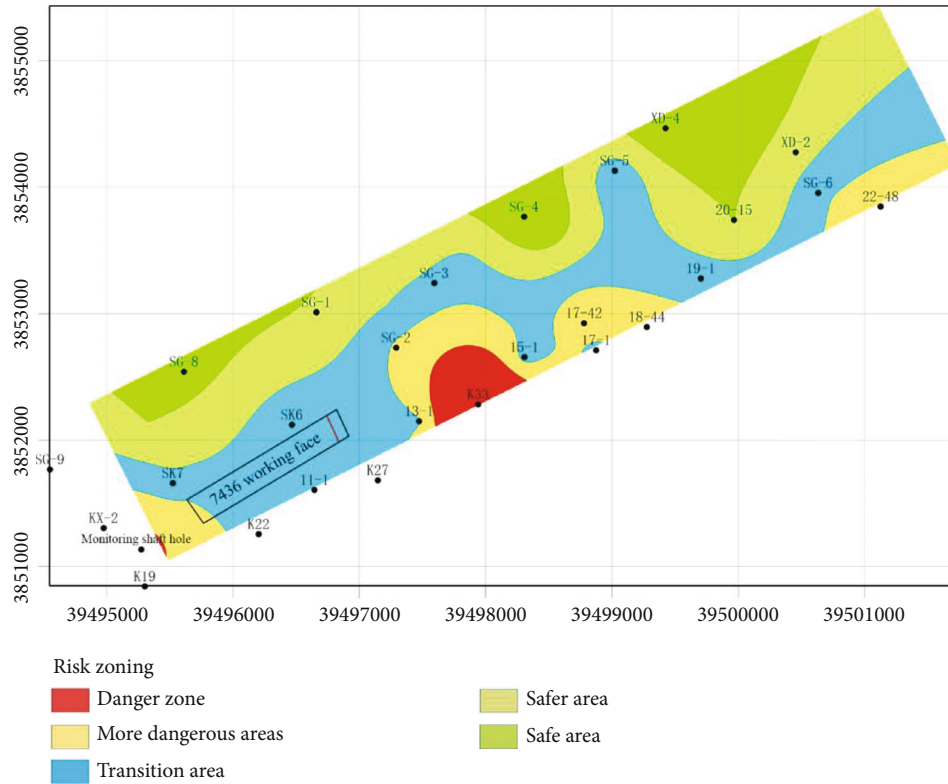


FIGURE 16: Zoning diagram of water inrush risk in Roof of No.7 coal seam.

roof water inrush risk index value thematic map is counted and graded, so as to obtain a best classification state and achieve the smallest difference within the group and the largest difference between the groups. The classification results are shown in Figure 15.

The best water inrush hazard index (TS) classification thresholds at all levels are 0.36, 0.44, 0.51, and 0.60, respectively. According to each classification threshold, the risk of water inrush from the roof of the no. 7 coal seam in the study area is divided into five types, as shown in Table 2.

According to the classification results, the zoning map for evaluating the risk of water inrush from the roof of the no. 7 coal seam in the area is obtained, as shown in Figure 16. According to the zoning results, most of the 7436 working face is in the transition zone, and only the area near the incision hole is at a relatively high level of the danger zone. The K33 borehole and surrounding areas in the entire deep research area are in the danger zone of water inrush from the roof and need to be guarded against. The normal water inflow is expected to be 15 m³/h, and the maximum water inflow is 30 m³/h during normal mining of the working face.

5. Conclusions

The advantages of this study are that the temporal and spatial evolution mechanism of the water-conducting fractured zone of overlying strata in the Kongzhuang coal mine is revealed, and the disadvantages of this study are that the temporal and spatial evolution mechanism of the water-

conducting fractured zone of overlying strata in other mining conditions is not clear, which should be researched systematically. The limitations of this study are that the temporal and spatial evolution mechanisms of the water-conducting fractured zone of overlying strata in other mining conditions are not researched. The effect of this study on practical projects and the benefits for future development are that the research results can provide the theoretical guidance for the prediction and prevention of water inrush disaster in the coal mine. The main conclusions in this research are as follows:

- (1) The main water filling sources affecting the #7 coal seam are sandstone water at the boundary of the Lower Shihezi Formation and sandstone fissure water at the roof of the Shanxi Formation. The water-filling channel formed by mining activities is the most important water-filling channel for mine water filling. The coarse sandstone (7.71 m), which is 64.76 m away from #7 coal, is the main key layer; mudstone (5.93 m), mudstone (6.56 m), which is 27.75 m away from #7 coal, and mudstone (7.65 m) 35.94 m away from coal seam 7, are sub key layers. The sandy rock stratum is thin, and the sandy mudstone with large thickness has an obvious control effect on the development of a water-conducting fractured zone
- (2) The caving zone is 26.7 m, which is about 8.3 times of the mining height. The fracture height is 68.3 m,

which is about 16.26 times of the mining height. The caving angle at the cut is 58.3, and the caving angle at the stop mining line is 57.2. With the advance of the working face, the crack density value gradually increases before the first weighing. During the first weighting, the crack density decreases continuously in the middle of the gob. The development law of “two zones” in the overburden of 7303 working face is detected by monitoring the loss of the borehole. Specifically, the self-designed double-end water shut-off is employed to detect the development height of the two zones and improve the observation method of borehole leakage

- (3) The height of the water-conducting fractured zone is determined accurately by field detection and analysis. The results of the loss of #1 and #2 boreholes show that the height of the water-conducting fractured zone is 63.70–65.27 m, and the split-mining ratio is 15.17 : 15.54. Using the method of GIS and AHP (analytic hierarchy process), the risk division of water inrush of coal seam roof is carried out in deep area. The results show that most of the deep working face 7436 is in the transition zone, and a small area around the cutting face is in the more dangerous zone. The research results provide the theoretical guidance for the prediction and prevention of water inrush disaster in the coal mine

Data Availability

The data used to support the findings of this study are included within the article.

Conflicts of Interest

The authors declare that they have no conflicts of interest.

Acknowledgments

This work was supported by the National Natural Science Foundation of China (52004082, 52174073, and 52274079), the Program for the Scientific and Technological Innovation Team in Universities of Henan Province (23IRTSTHN005), the Natural Science Foundation of Henan Province (222300420007), and the Project of Henan Key Laboratory of Underground Engineering and Disaster Prevention (Henan Polytechnic University).

References

- [1] L. M. Fan, X. D. Ma, Z. Q. Jiang, K. Sun, and R. J. Ji, “Review and thirty years prospect of research on water-preserved coal mining,” *Coal Science and Technology*, vol. 47, no. 7, pp. 1–30, 2019.
- [2] Q. B. Huang, J. B. Peng, Y. F. Wang, and N. N. Liu, “Issues and challenges in the development of urban underground space in adverse geological environment,” *Earth Science Frontiers*, vol. 26, no. 3, pp. 85–94, 2019.
- [3] J. L. Xu, “Research and progress of coal mine green mining in 20 years,” *Coal Science and Technology*, vol. 48, no. 9, pp. 1–15, 2020.
- [4] J. H. Wang, S. C. Li, L. P. Li, and Z. H. Xu, “Dynamic evolution characteristics and prediction of water inflow of karst piping-type water inrush of tunnels,” *Chinese Journal of Geotechnical Engineering*, vol. 40, no. 10, pp. 1880–1888, 2018.
- [5] D. Ma, H. Duan, Q. Zhang et al., “A numerical gas fracturing model of coupled thermal, flowing and mechanical effects,” *Computers, Materials & Continua*, vol. 65, no. 3, pp. 2123–2141, 2020.
- [6] D. Ma, H. Duan, and J. Zhang, “Solid grain migration on hydraulic properties of fault rocks in underground mining tunnel: radial seepage experiments and verification of permeability prediction,” *Tunnelling and Underground Space Technology*, vol. 126, article 104525, 2022.
- [7] Z. Huang, S. J. Li, K. Li, R. Wu, and W. Zhong, “Water inrush mechanism for slip instability of filled karst conduit in tunnels,” *Journal of Central South University (Science and Technology)*, vol. 50, no. 5, pp. 1119–1126, 2019.
- [8] H. G. Zhang, G. Z. Zhang, and B. Y. Mao, “Mechanism analysis and water and mud breakout in the Xiaogao mountain tunnel in Shanghai-Kunming passenger dedicated railway,” *Journal of Railway Engineering Society*, vol. 33, no. 8, pp. 66–70, 2016.
- [9] Z. Z. Shen, F. Chen, and J. Zhao, “Experimental study on seepage characteristics of the intersection of tubular karst passage and fissure,” *Journal of Hydraulic Engineering*, vol. 39, no. 2, pp. 137–145, 2008.
- [10] J. Q. Guo, G. Y. Wang, and L. W. Ren, “Karst geological features of Yiwan line and their basic modes,” *The Chinese Journal of Geological Hazard and Control*, vol. 24, no. 2, pp. 72–78, 2013.
- [11] J. L. Xu, X. Z. Wang, W. T. Liu, and Z. G. Wang, “Effects of primary key stratum location on height of water flowing fracture zone,” *Chinese Journal of Rock Mechanics and Engineering*, vol. 28, no. 2, pp. 380–385, 2009.
- [12] L. Q. Shi, X. G. Yu, J. C. Wei et al., “An analysis of factors affecting water-inrush from the number 4 coal seam roof conglomerate in the Huafeng coal mine,” *Journal of China University of Mining & Technology*, vol. 39, no. 1, pp. 26–31, 2010.
- [13] J. L. Xu, W. B. Zhu, and X. Z. Wang, “New method to predict the height of fractured water-conducting zone by location of key strata,” *Journal of China Coal Society*, vol. 37, no. 5, pp. 762–769, 2012.
- [14] X. H. Chen, C. Y. Liu, and J. X. Yang, “Study on influence law of stope roof movement to roof water gush,” *Coal Engineering*, vol. 46, no. 9, pp. 67–72, 2014.
- [15] X. C. Gao and Y. P. Wu, “Water-inrush risk and control technology in extra-thick seam of water-rich overburden,” *Safety in Coal Mines*, vol. 45, no. 1, pp. 54–56, 2014.
- [16] Q. Wu, K. Xu, and W. Zhang, “Further research on ‘three maps-two predictions’ method for prediction on coal seam roof water bursting risk,” *Journal of China Coal Society*, vol. 41, no. 6, pp. 1341–1347, 2016.
- [17] Y. F. Zeng, Z. Li, H. J. Gong, and J. H. Zheng, “Water abundance characteristics in aquifer of weathered roof bedrock and prediction on water inrush risk,” *Coal Engineering*, vol. 50, no. 2, pp. 100–104, 2018.
- [18] K. Sun, Y. C. Xia, C. Li, J. P. Chen, and G. Fang, “Risk assessment of water inflow (inrush) from coal seam roof under fully

- mechanized caving mining,” *Journal of Xi’an University of Science and Technology*, vol. 39, no. 3, pp. 452–460, 2019.
- [19] Z. G. Cao, J. F. Ju, and J. L. Xu, “Distribution model of water-conducted fracture main channel and its flow characteristics,” *Journal of China Coal Society*, vol. 44, no. 12, pp. 3719–3728, 2019.
- [20] W. G. Du, J. Chai, D. D. Zhang, and W. L. Lei, “Optical fiber sensing and characterization of water flowing fracture development in mining overburden,” *Journal of China Coal Society*, vol. 46, no. 5, pp. 1565–1575, 2021.
- [21] Y. Zhang, S. Cao, L. Lan, R. Gao, and H. Yan, “Analysis of development pattern of a water-flowing fissure zone in short-wall block mining,” *Energies*, vol. 10, no. 5, p. 734, 2017.
- [22] C. Zheng, L. Yu, N. Sun, H. Zhou, and J. He, “Size effect of water-flowing fracture zone height based on FLAC^{3D},” *E3S Web of Conferences*, vol. 194, article 01011, 2020.
- [23] T. D. Zhang, H. B. Wu, and K. K. Ren, “Height prediction and factor analysis of water fracture zone based on MNR,” *International Core Journal of Engineering*, vol. 6, no. 9, pp. 163–173, 2020.
- [24] Y. Xue, J. Liu, P. G. Ranjith, F. Gao, H. Xie, and J. Wang, “Changes in microstructure and mechanical properties of low-permeability coal induced by pulsating nitrogen fatigue fracturing tests,” *Rock Mechanics and Rock Engineering*, vol. 55, no. 12, pp. 7469–7488, 2022.
- [25] Z. Cao, Y. Wang, H. Lin, Q. Sun, X. Wu, and X. Yang, “Hydraulic fracturing mechanism of rock mass under stress-damage-seepage coupling effect,” *Geofluids*, vol. 2022, Article ID 5241708, 11 pages, 2022.
- [26] Y. Xue, P. G. Ranjith, Y. Chen, C. Cai, F. Gao, and X. Liu, “Nonlinear mechanical characteristics and damage constitutive model of coal under CO₂ adsorption during geological sequestration,” *Fuel*, vol. 331, article 125690, 2023.
- [27] Y. Xue, J. Liu, P. G. Ranjith, F. Gao, Z. Zhang, and S. Wang, “Experimental investigation of mechanical properties, impact tendency, and brittleness characteristics of coal mass under different gas adsorption pressures,” *Geomechanics and Geophysics for Geo-Energy and Geo-Resources*, vol. 8, no. 5, p. 131, 2022.
- [28] A. Gang-jian, C. Zheng-zheng, D. Hong-fei, L. Guo-sheng, and L. Ao, “Mechanical response of surrounding rock of Karst tunnel under stress-damage-seepage coupling effect,” *Geofluids*, vol. 2022, Article ID 6879808, 11 pages, 2022.
- [29] Y. Xue, J. Liu, X. Liang, S. Wang, and Z. Ma, “Ecological risk assessment of soil and water loss by thermal enhanced methane recovery: numerical study using two-phase flow simulation,” *Journal of Cleaner Production*, vol. 334, article 130183, 2022.
- [30] W. Wang, Z. Li, J. Xu, Y. Wang, X. Fan, and S. Li, “Evolution mechanism of water-conducting fissures in overlying rock strata with karst caves under the influence of coal mining,” *Geofluids*, vol. 2022, Article ID 4064759, 11 pages, 2022.
- [31] J. Tian, G. M. Dong, and L. C. Shu, “Research on relationship between parameters and attenuation coefficients of pore-pipe underground river systems, Southwest China,” *Hydrogeology and Engineering Geology*, vol. 40, no. 2, pp. 13–18, 2013.
- [32] D. Ma, J. Zhang, H. Duan et al., “Reutilization of gangue wastes in underground backfilling mining: overburden aquifer protection,” *Chemosphere*, vol. 264, article 128400, 2021.
- [33] X. Y. Wang, Z. S. Tan, M. S. Wang, and M. Q. Zhang, “Study on the waterproof and drainage principle and technology for karst tunnels on Yichang-Wanzhou railway,” *Engineering Science*, vol. 12, no. 8, pp. 107–112, 2010.
- [34] Y. Xue, S. Liu, J. Chai et al., “Effect of water-cooling shock on fracture initiation and morphology of high-temperature granite: Application of hydraulic fracturing to enhanced geothermal systems,” *Applied Energy*, vol. 337, Article ID 120858, 2023.
- [35] L. Xiao-Lei, L. Xin-Lei, W. Yue et al., “The seepage evolution mechanism of variable mass of broken rock in karst collapse column under the influence of mining stress,” *Geofluids*, vol. 2023, Article ID 7256937, 10 pages, 2023.
- [36] Y. Xue, P. G. Ranjith, F. Gao, Z. Zhang, and S. Wang, “Experimental investigations on effects of gas pressure on mechanical behaviors and failure characteristic of coals,” *Journal of Rock Mechanics and Geotechnical Engineering*, vol. 15, no. 2, pp. 412–428, 2023.
- [37] H. Dian-chen, S. Xiao-jian, W. Wen-qiang, D. Feng, and Z. Yu-yao, “Water inrush mechanism in fault fracture zone based on a nonlinear mechanical model of three flow fields,” *Geofluids*, vol. 2023, Article ID 4743053, 9 pages, 2023.
- [38] Y. Xue, J. Liu, X. Liang et al., “Influence mechanism of brine-gas two-phase flow on sealing property of anisotropic caprock for hydrogen and carbon energy underground storage,” *International Journal of Hydrogen Energy*, vol. 48, no. 30, pp. 11287–11302, 2023.